Nonisothermal gravitational segregation by molecular dynamics simulations

Guillaume Galliéro[1,*] and François Montel[2]
[1]*Laboratoire des Fluides Complexes (UMR-5150 with CNRS), Université de Pau et des Pays de l'Adour, BP 1155, F-64013 Pau Cedex, France*
[2]*TOTAL S.A., avenue Larribau, F-64018 Pau Cedex, France*
(Received 4 August 2008; published 22 October 2008)

In this work, a molecular dynamics algorithm is proposed to study the transient and the stationary state of gravitational segregation in simple fluid mixtures. Both isothermal and stable nonisothermal (where thermodiffusion occurs) cases have been studied. This approach is applied extensively on a simple fluid model: Lennard-Jones mixtures composed of species differing only in their masses. First, using isothermal binary equimolar mixtures, it is shown that the molecular dynamics simulations provide stationary results consistent with the thermodynamic modeling in various thermodynamic conditions and for different gravity fields. Next, in stable nonisothermal mixtures heated from below, it is shown that the gravitational segregation and the thermodiffusion process (Soret effect) have an opposite effect on the concentration profiles along the fluid column. Then, molecular dynamics simulations are performed on ternary and ten-component mixtures. For these multicomponent nonisothermal mixtures, results obtained emphasize the fact that the way the thermodiffusion is estimated should be done with care. In addition, for all nonisothermal configurations, the simulation results confirm that the thermodiffusion may have a non-negligible influence on the concentration profile in a petroleum reservoir. Finally, by analyzing the transient behavior during the molecular dynamics simulations, it is shown that the dynamic of the gravitational segregation is unambiguously controlled by the mass diffusion.

DOI: 10.1103/PhysRevE.78.041203 PACS number(s): 66.10.cd, 47.11.Mn, 05.70.Ln

I. INTRODUCTION

A precise knowledge of the initial state of a petroleum reservoir is crucial in order to optimize its development plan. Such knowledge relies on the ability of describing correctly the spatial distribution of the hydrocarbons which is mainly modeled by the gravity field through the gravitational segregation [1–4]. In fact, just by adding the gravity contribution to the chemical potential (described by an *ad hoc* thermodynamic model), it is possible to estimate the composition of the fluid column from the one at a reference depth. Nevertheless, in many fields, the compositional profile computed so differs from the actual one. So, one has to introduce other external forces that may occur such as the thermal field, external fluxes, chemical reactions, etc. But a complete picture is hard to achieve, especially in formulating the dynamic of the evolution of the compositional profile, even if recent improvements have been achieved [5–7].

One system of interest to improve the species distribution estimation in a reservoir is the situation where only gravitational and geothermal (through the thermodiffusion effect) forces occur in a convection free configuration. In such a case, gravitational segregation and thermodiffusion (the Soret effect) generally induce opposite effects on the distribution of the species along the reservoir [7,8]. This is the case, for instance, when linear alkanes are involved. Gravity tends to increase the concentration of the longest chains in the bottom of the reservoir whereas the effect of thermodiffusion is opposite. Nevertheless, the accurate modeling of the steady state nonisothermal gravitational segregation is not simple to deal with in multicomponent mixtures. This is by part due to the lack of knowledge of the coefficients characterizing the thermodiffusion (the Soret effect), even if there are recent improvements in measuring this transport property in hydrocarbon mixtures [9–11].

In this work, for the first time ever to the best of our knowledge, it is proposed to use molecular dynamics (MD) simulations on Lennard-Jones (LJ) spheres in order to study gravitational segregation in isothermal and nonisothermal "isotopic" mixtures, i.e., analyze the coupling between the gravity field and thermodiffusion effects on the composition profiles in simple ideal mixtures. Throughout the text, an "isotopic" mixture means a system for which only the masses differ between the components. In addition, we point out here that the mass ratios between the species employed here (up to 10) are by far larger than the mass ratio encountered in real isotopes.

Such a molecular dynamics approach to tackle nonisothermal gravitational segregation is interesting in complement to the macroscopic modeling for four main reasons:

(i) It does not assume explicitly the underlying formalism to describe this process and so allows a true "test" of the phenomelogical macroscopic theory usually used.

(ii) It permits the description of not only the stationary state but also the transient toward this state which is not accessible using thermodynamic modeling.

(iii) Contrary to the macroscopic model, the physical properties, including the thermodiffusion coefficients, are not inputs of the simulation but results for a given fluid model.

(iv) Because of the vertical size involved (typically 10 nm) in the simulation, the Rayleigh number is always largely smaller than its critical value even when heating strongly from below, i.e., the fluid column remains always in a stable regime (no convection occurs).

*Corresponding author. FAX: +33 5 59 40 7695. guillaume.galliero@univ-pau.fr

In the first part, the thermodynamic modeling of isothermal and nonisothermal gravitational segregation is described. For the particular case of stable isotopic mixtures, the analytical solution of the stationary concentration profile is then provided. In addition is described the proposed MD algorithm to simulate nonisothermal gravitational segregation together with some numerical details on the simulations. Then, in a second part, the results of the MD simulations for various configurations are presented, discussed, and compared with the thermodynamic modeling. After some preliminary results, the proposed MD algorithm is utilized in simple isothermal isotopic binary mixtures subject to different gravity fields and for various thermodynamic conditions. Next, nonisothermal gravitational MD simulations (in which gravitational segregation and thermodiffusion compete) are presented for various thermal gradients. Results on ternary and ten-component isotopic mixtures are then given and compared to the thermodynamic modeling with a particular emphasis on how thermodiffusion should be described in such systems. Finally, in the frame of a mass diffusion process the MD results of the transient state behavior of isothermal and nonisothermal gravitational segregation are presented and discussed.

II. THEORY

A. Isothermal gravitational segregation

When an isothermal N-component mixture is subject to a constant gravity field (directed along the z direction which is chosen to be positive downward), at equilibrium, the distribution of the species i can be deduced from the fact that the total potential of each component is constant [12]:

$$\left(\frac{d\mu_i}{dz}\right)_T = M_i g, \tag{1}$$

where μ_i is the chemical potential, T is the temperature, M_i is the molecular weight, and g is the gravitational acceleration.

This equation, given a composition at a reference point z^0, can be used to obtain the variation of composition (due to the gravitational segregation) at the stationary state as a function of depth. For most systems, Eq. (1) cannot be solved analytically and a thermodynamic modeling combined with a numerical procedure has to be employed [2,3,13]. Nevertheless, for the systems studied here, isotopic mixtures, Eq. (1) can be solved analytically. To obtain this analytical solution, we start from the fact that, in an isothermal N-component mixture,

$$d\mu_i = v_i dp + \sum_{j=1}^{N-1} \frac{\partial \mu_i}{\partial x_j} dx_j, \tag{2}$$

where v_i and x_i are, respectively, the molar volume and the molar fraction of component i and p is the pressure. Using the fact that isotopic mixtures are ideal ones [14],

$$\mu_i = RT \ln x_i + \text{const}, \tag{3}$$

where R is the gas constant, Eq. (2) can be rewritten as

$$d\mu_i = v_i dp + RT\frac{dx_i}{x_i}. \tag{4}$$

In addition, the hydrostatic equilibrium implies that

$$\frac{dp}{dz} = \rho g, \tag{5}$$

where ρ is the density. By combining Eqs. (1), (4), and (5), we obtain an equation similar to that of Svedberg [15]:

$$\frac{dx_i}{x_i} = \frac{g}{RT}(M_i - v_i\rho)dz. \tag{6}$$

Furthermore, in an isotopic mixture, we have simply

$$v_i\rho = x_i M_i + (1 - x_i)M_x, \tag{7}$$

where

$$M_x = \frac{1}{1 - x_i}\sum_{j\neq i}^{N} x_j M_j. \tag{8}$$

This allows us to rewrite Eq. (6) as

$$\frac{dx_i}{x_i(1 - x_i)} = \frac{g}{RT}(M_i - M_x)dz. \tag{9}$$

Equation (9) can be integrated from a reference depth z^0 for which the molar fraction x_i^0 is known. This integration provides the stationary variation of composition of component i vs the depth when dealing with an isotopic mixture (or an ideal gas one):

$$x_i = \frac{(x_i^0/1 - x_i^0)\exp[(g/RT)(M_i - M_x)(z - z^0)]}{1 + (x_i^0/1 - x_i^0)\exp[(g/RT)(M_i - M_x)(z - z^0)]}. \tag{10}$$

B. Nonisothermal gravitational segregation

The problem is by far more complex when, in addition to the gravity field, the system is subject to a thermal gradient directed along the z axis. If the fluid column is heated from below, namely the Rayleigh-Bénard configuration, the system may be unstable and convection may occur [16]. In pure fluid, with a negligible pressure gradient, the stability of such a configuration is governed by the Rayleigh number

$$Ra = \frac{\alpha_p \Delta T g h^3}{\nu\kappa}, \tag{11}$$

where α_p is the thermal expansion coefficient of the fluid, ΔT is the temperature difference over the height of the fluid column h, ν is the kinematic viscosity, and κ is the thermal diffusivity. For a pure fluid located between two horizontal impermeable walls, the system is stable, i.e., in the diffusive regime, while $Ra < Ra_c = 1708$ [16]. In a more than two component mixture, the stability analysis becomes very hard to achieve properly [17]. In fact, in a segregated N-component mixture, over a large fluid column, one should take into account as well the concentration and the pressure gradients to perform a complete stability analysis [7,18]. These contributions will not be considered in this study.

In a stable system, because of the presence of a thermal gradient, thermodiffusion may occur and may modify the composition profiles from the ones due to gravitational segregation alone [6–8]. To characterize thermodiffusion, we define a "generalized" thermal diffusion factor of component i, as in Kempers [19]:

$$\alpha_{T_i} = -\frac{T}{x_i(1-x_i)}\frac{\nabla x_i}{\nabla T}. \tag{12}$$

Using this formulation, because of thermodiffusion, Eq. (9) becomes

$$\frac{dx_i}{x_i(1-x_i)} = \frac{g}{RT}(M_i - M_x)dz - \frac{\alpha_{T_i}}{T}dT. \tag{13}$$

In a previous work on LJ isotopic mixtures [20], we have shown that, for such mixtures, the thermal diffusion factor is independent of the temperature for a given density (contrary to the Soret coefficient $S_T = \alpha_T / T$) and is weakly dependent of the molar fraction. Thus, assuming that α_{T_i} is independent of both x_i and T, from Eq. (13) we obtain the composition profiles of an N-component isotopic mixture at the stationary state induced by nonisothermal gravitational segregation:

$$x_i = \frac{(x_i^0/1-x_i^0)\exp[(g/RT^0)(M_i - M_x)(z-z^0) - \alpha_{T_i}\ln(T/T^0)]}{1 + (x_i^0/1-x_i^0)\exp[(g/RT^0)(M_i - M_x)(z-z^0) - \alpha_{T_i}\ln(T/T^0)]}, \tag{14}$$

where T^0 is the temperature at the reference depth z^0.

C. Fluid model

To describe interaction between fluid particles (spheres), the classical truncated Lennard-Jones 12-6 potential has been used during the MD simulations:

$$U_{LJ} = 4\varepsilon\left[\left(\frac{\sigma}{r}\right)^{12} - \left(\frac{\sigma}{r}\right)^{6}\right], \tag{15}$$

where σ is the distance at which the potential is equal to zero (the "atomic diameter"), ε is the potential depth, and r is the intermolecular distance. A cutoff radius equal to 2.5σ has been used.

In the following, dimensionless quantities, denoted with a star as a superscript, have been used. σ has been employed as the length parameter, ε as the energy parameter, and M as the mass parameter.

D. Molecular dynamics scheme to simulate gravitational segregation

In order to simulate the gravitational segregation process by MD, a simple procedure has been developed. At both ends (along the vertical direction), two softly repulsive walls are added to the simulation box; see Fig. 1. Each wall interacts with the fluid particle through a Weeks-Chander-Andersen potential [21], i.e., a LJ potential truncated at the distance which corresponds to its minimum:

$$U_{wall} = 4\varepsilon\left[\left(\frac{\sigma}{d}\right)^{12} - \left(\frac{\sigma}{d}\right)^{6}\right] + \varepsilon, \quad d^* \leqslant 2^{1/6},$$

$$U_{wall} = 0, \quad \text{else} \tag{16}$$

where d^* is the distance from the wall.

The simulation box, which is divided in 20 slabs along the z axis, is noncubic with a large vertical extension; see Fig. 1. The vertical extension h^* has been chosen equal to 30, whereas horizontal, L_x^* and L_y^*, ones have been taken equal to 10. Such vertical extension is necessary in order to find a compromise between minimizing possible geometric confinement effects on the fluid structure or dynamic introduced by the walls (molecular packing [22]) and reasonable simulation duration. It should be noted that, due to the presence of walls and the fluid ordering so introduced, the three slabs located next to both walls (i.e., slabs 1, 2, 3 and 18, 19, 20) have been discarded from the analysis.

Once having equilibrated the system, a gravity potential $(-Mgz)$ applied on each particle is progressively increased from zero to its desired value during 10^4 time steps. Then, the gravity potential is kept constant at its final value and,

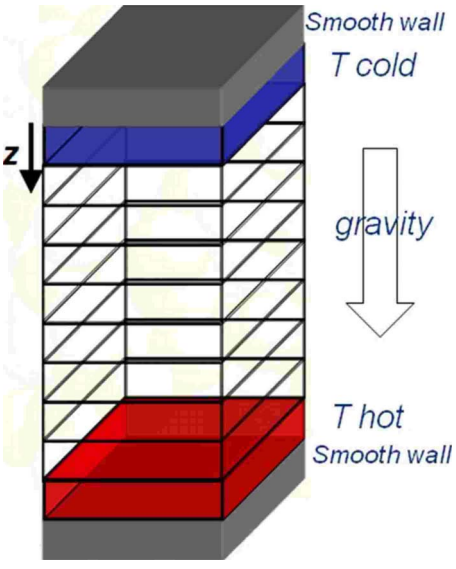

FIG. 1. (Color online) Schematic sketch of the simulation box used to perform MD computation of nonisothermal gravitational segregation.

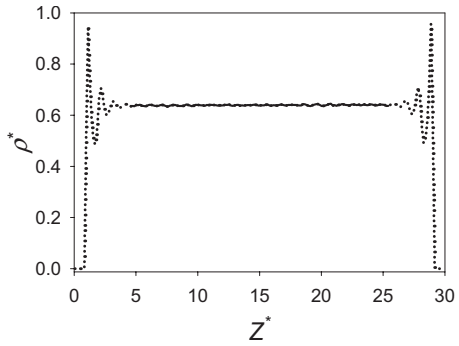

FIG. 2. Density profile along the vertical direction at $T^*=2$ and $\rho^*=0.6$. The full line represents the domain used to perform the analysis.

after a transient state, gravitational segregation established itself.

Concerning the imposition of the thermal gradient, a procedure similar to the one proposed by Müller-Plathe [23] has been employed. This approach consists of swapping every A time step (A ranging from 50 to 300) the "coldest" particle (i.e., the one with the lowest kinetic energy) located in slab 20 with the "hottest" one located in slab 1. Such a procedure consists of a simple redistribution of the kinetic energy within the simulation box. After a transient state, related to the thermal diffusivity, a thermal gradient establishes itself which allows thermodiffusion to occur in mixtures.

In order to compare the composition profile with the thermodynamic modeling, Eqs. (10) and (14), the reference values have been taken at the middle of the fluid column ($z^{0*}=h^*/2=15$). The reference molar fraction x_i^0 and temperature T^0 have been deduced from a linear interpolation of the MD results in slabs 10 and 11.

E. Simulation details

MD Simulations have been performed using a homemade code. Systems composed of 900 ($\rho^*=0.3$) to 1800 ($\rho^*=0.6$) particles have been used. Classical periodic boundary conditions (for both x and y directions, but not for the z direction), combined with a Verlet neighbors list have been applied [24]. A time step δ_t^* equal to 0.002 has been employed. To integrate the equation of motion, the velocity Verlet algorithm is used. To maintain the desired temperature during simulations, a Berendsen [25] thermostat with a large time constant equal to $1000\delta_t^*$ has been utilized. Discarding the transient state, about 10^6 time steps depending on the mixture and the state, nonequilibrium data have been collected during very long runs of $0.15-1\times10^8$ time steps. In order to estimate errors on the variables computed, the subblock average method has been applied [26].

It should be noted that the density values ρ^* are defined using the whole simulation box volume ($L_x^*\times L_y^*\times h^*$). Nevertheless, due to excluded volumes close to both walls, see Fig. 2, the "true" (bulk) density of the fluid phase is somewhat larger, roughly of the order of 30/28 higher.

III. RESULTS

A. Preliminary results

In a first step, we have performed a simulation on an isothermal pure fluid without gravity at $T^*=2.0$ and $\rho^*=0.6$. This thermodynamic state, a dense supercritical gas ($T_r=T/T_c\approx1.5$ and $\rho_r=\rho/\rho_c\approx2$, where T_c and ρ_c are, respectively, the critical temperature and the critical density of the LJ fluid [27]), corresponds to the condition for which most of the segregation MD simulations are performed in this work.

As expected, see Fig. 2, despite the purely repulsive nature of the two soft walls, the density profile along the vertical dimension (z) is not constant. The fluid exhibits a strong structure close to the walls which is due to the molecular packing effect [22]. Nevertheless, as shown in Fig. 2, the area on which the analysis is done, between slabs 4 and 16 (i.e., between $z^*=4.575$ and $z^*=25.425$), is not largely affected by the walls presence. In addition, as mentioned previously, because of the exclusion zone close to the walls, the bulk density is somewhat larger than 0.6, being equal to ~0.639.

For the same thermodynamic state, we have performed separate equilibrium and nonequilibrium MD simulations in order to estimate the physical properties that are needed to evaluate the Rayleigh number, Eq. (11). It should be noted that our MD code has already been validated for the computations of all these properties [28,29]. Using equilibrium MD simulations [30], we have obtained $\alpha_p^*=0.23\pm0.01$ and for the isobaric heat capacity $c_p^*=3.4\pm0.2$. In addition, using the boundary driven nonequilibrium scheme of Müller-Plathe [31], we have computed that the dynamic viscosity η^* is equal to 0.99 ± 0.04 and that the thermal conductivity λ^* is equal to 4.4 ± 0.2. Using these results, we can deduce that, for $\rho^*=0.6$, $T^*=2$, and $h^*=30$,

$$Ra\approx2.10^3\Delta T^*g^*. \tag{17}$$

This implies that if $\Delta T^*g^*\ll1$, then $Ra<Ra_c$ and the system simulated is stable. It should be mentioned that Eq. (17) provides only an approximation of the Rayleigh number in mixtures. First, it omits the concentration and the pressure gradient contributions (see Sec. II B). Second, the dimensionless transport properties (in particular, the thermal conductivity because of multiple definitions [15]) may be slightly different in mixtures compared to the pure fluid values [32,33].

B. Isothermal stationary gravitational segregation of binary mixtures

1. Influence of the gravity amplitude

In order to test the limitations of the proposed MD algorithm to simulate gravitational segregation, we have first simulated an isothermal binary equimolar isotopic mixture, for which $M_2/M_1=10$, subjects to various gravity amplitude. The thermodynamic conditions chosen are $T^*=2.0$ and $\rho^*=0.6$. The gravity acceleration $g^*=g\Sigma_{i=1}^N\frac{x_iM_i\sigma}{\varepsilon}$ has been changed from 0.01 to 0.32.

As expected, see Fig. 3, whatever g^*, the lightest compound is enriched at the top of the column (small z^* values).

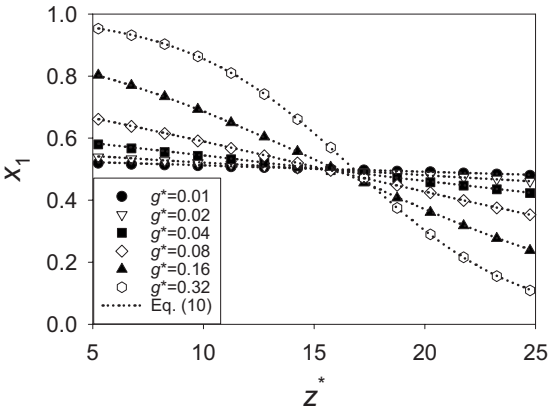

FIG. 3. Molar fraction stationary segregated profile of the lightest compounds in a binary equimolar isotopic mixture ($M_2/M_1=10$) at $T^*=2$ and $\rho^*=0.6$ under various gravity fields. Error bars are smaller than the symbols and so are not represented here.

More important, results shown in Fig. 3 clearly indicate that the proposed scheme provides a steady state composition profile in perfect agreement with the thermodynamic modeling, Eq. (10). This is the case even in the situations in which the molar fraction profile is not linear as for $g^*=0.32$.

It should be noted that the gravity values employed here are indeed large compared to what occurs in a petroleum reservoir. In fact, considering a mixture of methane with a "super" methane ($M_{\text{super-CH4}}=10M_{\text{CH4}}$), using the molecular parameters provided in Ref. [28], we obtain that the corresponding "real" heights h of the systems simulated (between $z^*=5.25$ and $z^*=24.475$) vary from 270 ($g^*=0.01$) to 8750 m ($g^*=0.32$)! These values should be compared with the usual petroleum reservoir height which generally varies from 100 to 1000 m.

2. Influence of the thermodynamic conditions

For the same isotopic mixture as in the previous section, we have evaluated the influence of the thermodynamic conditions, T^* and ρ^*, for a fixed gravity $g^*=0.02$. From the thermodynamic modeling, Eq. (10), the segregated concentration profile for the mixture studied here should be independent of the density. As a test, for $T^*=2$, we have changed ρ^* from 0.3 to 0.6 with a step of 0.1. Figure 4 clearly demonstrates that the segregated concentration profile provided by MD is independent of the initial density and is consistent with Eq. (10).

We have then changed the temperature keeping the density fixed at $\rho^*=0.6$. The temperatures studied are $T^*=0.9$, 1.5, 2, and 3. It should be noted that at $T^*=0.9$ the system is biphasic, see Fig. 5, the critical temperature of the truncated LJ fluid being located at $T_c^*\approx 1.1$ [34].

As previously, see Figs. 5 and 6, the MD results are consistent with those coming from the thermodynamic modeling, Eq. (10), and exhibit a more pronounced segregation when decreasing temperatures. In addition, it is worthwhile to note that in the biphasic case (see Fig. 3) the segregated concentration profile is not affected by the presence of an interface for such an isotopic mixture.

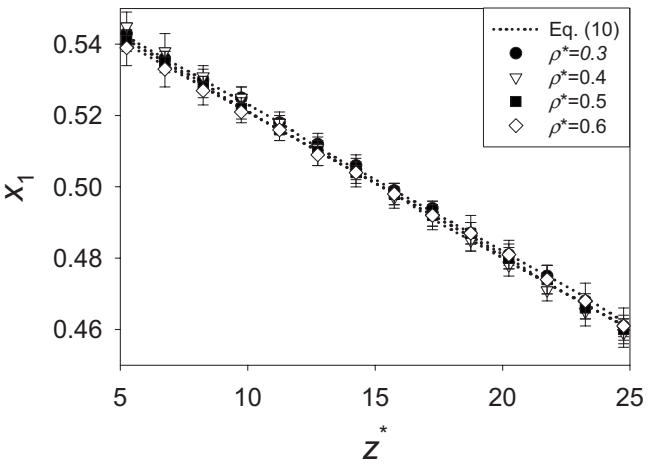

FIG. 4. Molar fraction stationary segregated profile of the lightest compounds in a binary equimolar isotopic mixture ($M_2/M_1=10$) at $T^*=2$ under $g^*=0.02$ for various densities.

C. Nonisothermal stationary cases

More complex are the cases in which a thermal gradient (along the z direction) is present in addition to the gravity field. In order to tackle this problem, we have performed MD simulations of the same equimolar isotopic mixture as in the previous section (at $T^*=2$ and $\rho^*=0.6$ on average) subject to a gravity field $g^*=0.02$ and to different thermal gradients $\Delta T^*/h^*$ taking the values 5.3×10^{-3}, 10.6×10^{-3}, 15.9×10^{-3}, and 21.2×10^{-3}. Considering the same methane plus "supermethane" mixture as in Sec. III B 1, the vertical extension of the column is about 550 m. Using these parameters, the corresponding "real" thermal gradient applied varies from 2.9 to 11.5 K per 100 m. Usually, the geothermal gradient at petroleum reservoir depths is of the order of 3 K per 100 m.

For the conditions applied here, the largest Rayleigh number, Eq. (17), corresponding to the largest ΔT^* value used, is below 30. So, its maximal value is largely below its critical threshold (Ra_c). Thus in all configurations studied here, the system is stable and only diffusion will occur. In fact, due to

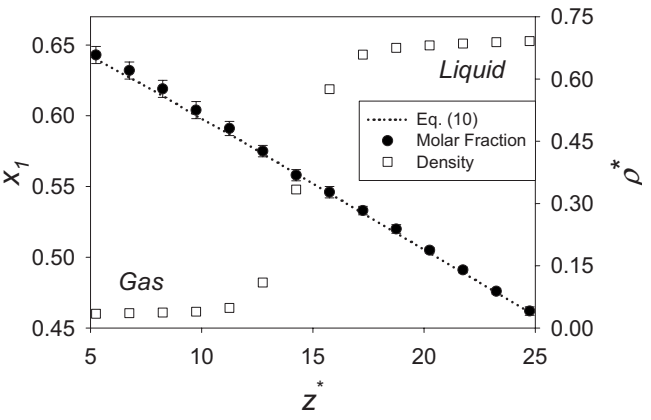

FIG. 5. Molar fraction and density stationary profiles in a binary equimolar isotopic mixture ($M_2/M_1=10$) at $T^*=0.9$ under $g^*=0.02$.

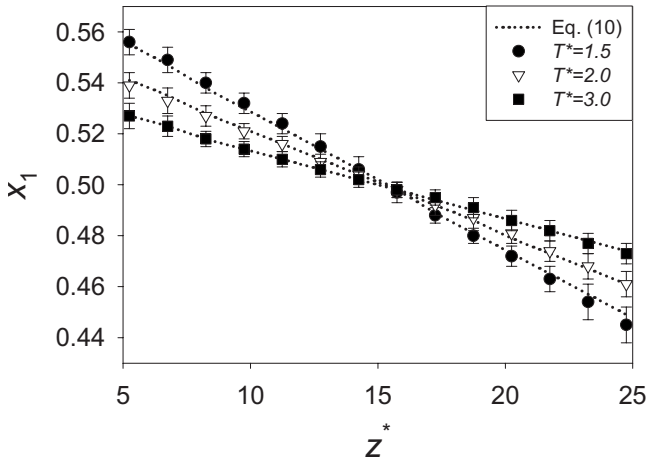

FIG. 6. Molar fraction stationary segregated profile of the lightest compound in a binary equimolar isotopic mixture ($M_2/M_1=10$) at $\rho^*=0.6$ under $g^*=0.02$ for various temperatures.

the very small system size accessible by MD simulations [appearing at the power of 3 in the definition of the Rayleigh number, Eq. (11)], a huge thermal gradient should be applied to destabilize the fluid column [35].

An example of the stationary density and temperature profiles of the segregated mixture is shown in Fig. 7. It is interesting to note that, for the largest thermal gradient, the density gradient is reversed, i.e., the density is larger at the top of the column than at the bottom; see Fig. 7. Nevertheless, despite this reverse density profile, the system is stable ($Ra < Ra_c$).

Because of the presence of a thermal gradient, the thermodiffusion process will take place in the simulation box in addition to the gravitational segregation. Therefore, one needs the value of the thermal diffusion factor of this mixture, α_T, in order to obtain the theoretical stationary molar fraction profile, Eq. (14). We have obtained this value using the correlation proposed in Galliero *et al.* [20], which has been developed for such LJ isotopic mixtures. For the systems studied here, this correlation yields $\alpha_T=2.08$. The fact that $\alpha_T>0$ indicates that the heaviest component tends to

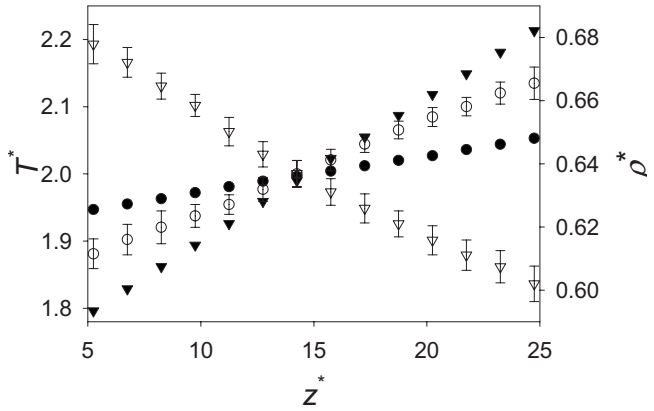

FIG. 7. Temperature (full symbols) and density (open symbols) stationary profiles of a binary equimolar isotopic mixture for $g^*=0.02$ and various thermal gradients (circles: $\Delta T^*/h^*=5.3\times10^{-3}$; down triangles: $\Delta T^*/h^*=21.2\times10^{-3}$).

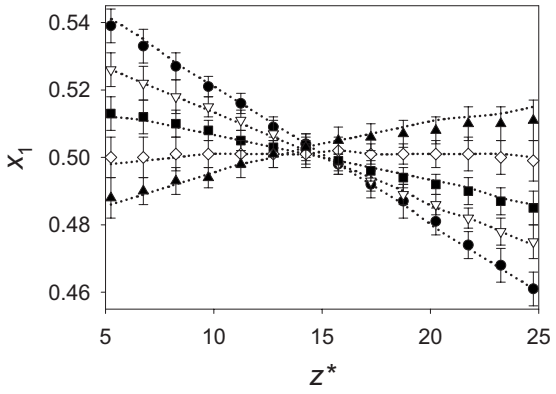

FIG. 8. Molar fraction stationary profiles of the lightest compound in a binary equimolar isotopic mixture for $g^*=0.02$ and various thermal gradients. The dotted lines correspond to the results of Eq. (14). Circles: $\Delta T^*/h^*=0$; down triangles: $\Delta T^*/h^*=5.3\times10^{-3}$; squares: $\Delta T^*/h^*=10.6\times10^{-3}$; diamonds: $\Delta T^*/h^*=15.9\times10^{-3}$; up triangles: $\Delta T^*/h^*=21.2\times10^{-3}$.

migrate towards the cold areas. Thus for the systems studied (heated from below), the thermodiffusion effect on the molar fraction profile is opposite the one induced by the gravitation field. It should be noted that such a α_T value is of the order of magnitude of those in simple hydrocarbon mixtures [9–11] but is rather small compared to those in colloids or nanofluids [36,37]. In addition, it has been shown in a previous work [20] that the amplitude of the thermal diffusion factor in normal-alkane binary mixtures can be correctly approximated by the mass contribution (isotopic) alone.

In Fig. 8, it clearly appears that the thermodiffusion effect can have a strong impact on the composition profile; the larger the thermal gradient the larger the influence of the thermodiffusion. For a large thermal gradient ($\Delta T^*/h^* > 1.5\times10^{-2}$), the composition distribution may even be reversed, i.e., the heaviest compound is enriched at the top of the fluid column! In addition, it is really interesting to note that, whatever the thermal gradient, Eq. (14) combined with the estimated α_T value provides results which are fully consistent with the MD simulations, see Fig. 8.

For a "realistic" thermal gradient ($\Delta T^*/h^*=5.3\times10^{-3}$), it is worthwhile to emphasize that, for the system studied here, the thermodiffusion impact on the concentration profiles is less pronounced than the gravity one but is not negligible at all; see Fig. 8. Keeping in mind that the thermodiffusion amplitude of the system studied here is not particularly important, the non-negligible thermodiffusion influence on the concentration distribution supports the fact that thermodiffusion had to be taken into account in order to obtain an accurate description of the fluid distribution in a petroleum reservoir at the initial state [6–8]. In addition, we can suspect that the thermodiffusion effect may even favor the apparition of an unstable situation in particular petroleum reservoirs.

D. Multicomponent mixture

In order to analyze the behavior of some multicomponent mixtures, we have performed simulations on ternary and ten-component isotopic mixtures at $T^*=2$ and $\rho^*=0.6$ for g^*

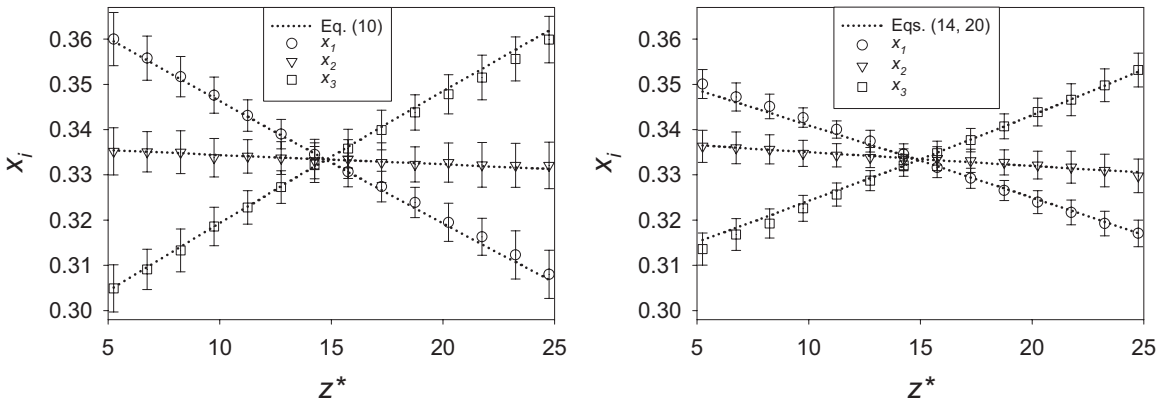

FIG. 9. Isothermal (left figure) and nonisothermal (right figure, $\Delta T^*/h^*=5.3\times10^{-3}$) molar fraction segregated profiles in a ternary isotopic mixture.

$=0.02$. For the ternary mixture the species masses are $M_3=2M_2=10M_1$ and for the ten-components one the species masses are $M_{10}=10M_1$, $M_9=9M_1$, …, $M_3=3M_1$, and $M_2=2M_1$. Both mixtures are equimolar ones, i.e., $x_i=x_j$.

In a first step, isothermal MD simulations have been performed for both mixtures. Results provided in Figs. 9 and 10 indicate that MD values and those yielded by the thermodynamic modeling, Eq. (10), are in a very good agreement (within the error bars) for both the ternary and the ten-component mixtures. It is worthwhile to mention that, for the ten-component mixture, despite an extremely long run (6×10^7 time steps), the error bars are rather large because of a low statistic when small values of molar fractions are used.

In a second step, we have performed MD simulations in non isothermal conditions using a "realistic" thermal gradient, $\Delta T^*/h^*=5.3\times10^{-3}$ for even longer runs (10^8 time steps). In such situations, to apply Eq. (14) in order to obtain the analytical nonisothermal segregated profiles, the thermal diffusion factor of each species i, α_{Ti}, should be estimated. To do so, it is necessary to first define a one fluid approximation on mass on all the compounds $j\neq i$ [21,38] to estimate the mass of the pseudospecies "equivalent" to the rest of the mixture and then to use the correlation provided in Galliero *et al.* [20]. However, this lumping process should respect the constraint that, in a N-components mixture;

$$\sum_{i=1}^{N} \nabla x_i = 0. \tag{18}$$

Equations (12) and (18) impose that, in a nonisothermal equimolar mixture ($x_i=x_j$) without gravitational segregation,

$$\sum_{i=1}^{N} \alpha_{T_i} = 0. \tag{19}$$

However, if the usual linear assumption is employed, i.e., using Eq. (8) as the one fluid approximation, the correlation of Galliero *et al.* [20] does not ensure the constraint imposed by Eq. (19); see Table I. In fact, Eq. (8) used as a one fluid approximation mass tends to overestimate the mass of the pseudospecies. In order to circumvent this inconsistency, we propose an empirical one fluid approximation on mass which writes, when dealing with a species i,

$$M_x^{3/2} = \frac{1}{(1-x_i)^2}\sum_{j\neq i}^{N}\sum_{k\neq i}^{N} x_j x_k \left(\frac{2M_jM_k}{M_j+M_k}\right)^{3/2}. \tag{20}$$

This equation is similar to the one used in some models developed for predicting viscosity in mixture (with an exponent of 1.5 instead of 0.5 [32]) and allows us to obtain smaller M_x than Eq. (8). Thermal diffusion factor values pro-

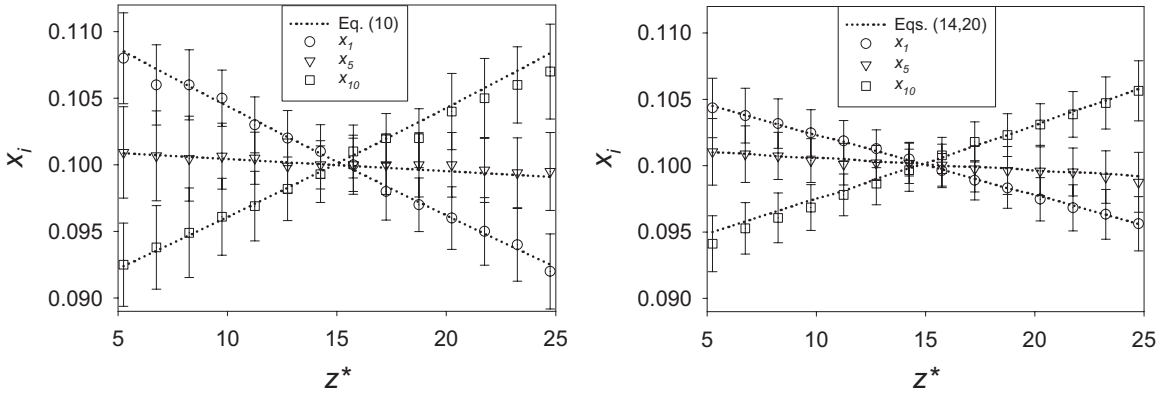

FIG. 10. Isothermal (left figure) and nonisothermal (right figure, $\Delta T^*/h^*=5.3\times10^{-3}$) molar fraction segregated profiles in a ten-component isotopic mixture (for the sake of readability, only profiles of components 1, 5, and 10 are shown).

TABLE I. Ternary and ten-component thermal diffusion factors of each compound, using Eq. (8) as the one fluid approximation on mass.

Mixture	α_{T1}	α_{T2}	α_{T3}	α_{T4}	α_{T5}	α_{T6}	α_{T7}	α_{T8}	α_{T9}	α_{T10}
Ternary	1.77	0.12	−1.46							
Decanary	1.46	1.08	0.73	0.42	0.13	−0.13	−0.36	−0.57	−0.75	−0.93

vided by this new one fluid approximation on mass are provided in Table II.

It is interesting to note that Eq. (19) is very well respected for both mixtures when this empirical one fluid approximation, Eq. (20), is used; see Table II. In addition, even if the differences between values provided in Tables I and II are generally not large, in some cases the thermal diffusion factor sign can be opposite, e.g., α_{T2} in the ternary mixture.

From the nonisothermal results shown in Figs. 9 and 10, it appears that the thermodynamic modeling, Eq. (14), coupled with the new one-fluid approximation, Eq. (20), is in excellent agreement with the MD simulations results for both the ternary and the ten-component mixtures. In addition, as for binary mixtures, the concentration profiles are modified in a noticeable manner by the thermodiffusion effect compared to the isothermal ones. This confirms the importance of thermodiffusion when estimating the concentration profile in petroleum reservoirs with a large vertical extension.

To emphasize the differences between the use of Eq. (8) or Eq. (20) as the one fluid model on mass, we have performed nonisothermal simulations of the same ternary mixture but subjected to a stronger thermal gradient, $\Delta T^*/h^* = 15.9 \times 10^{-3}$, in order to enhance the influence of the thermodiffusion.

Figure 11 shows that the choice of an adequate one fluid model on mass may affect noticeably the concentration profile predicted. In the example chosen, Eq. (14) combined with Eq. (8) predicts a homogeneous distribution of component 2 whereas Eq. (14) combined with the new Eq. (20) predicts an enrichment of component 2 at the top of the column. It is interesting to note that MD results and those predicted by Eq. (14) combined with the new one fluid approximation on mass, Eq. (20), are consistent; see Fig. 11. Such a good agreement cannot be achieved using Eq. (8) as the one fluid approximation on mass.

E. Transient behavior

One major advantage of the MD simulation is that it allows the analysis of the transient behavior of the gravitational segregation without postulating *a priori* how this segregation establishes itself. In order to study this transient behavior, we have performed MD simulations of an isotopic equimolar binary mixture ($M_2/M_1 = 10$) subject to $g^* = 0.02$ at $T^* = 2.0$ and $\rho^* = 0.6$. Both isothermal and nonisothermal ($\Delta T^*/h^* = 5.3 \times 10^{-3}$) cases have been simulated. To analyze this transient behavior, the molar fraction of component 1 has been measured (averaged on 50 time steps) during the transient in slab 17. In order to reduce, the statistical uncertainties, the results presented in Fig. 12 correspond to an average of 20 different independent runs.

Figure 12 shows that isothermal and nonisothermal molar fraction evolutions are very similar and both resemble a "diffusive" evolution. In order to relate this transient behavior to a diffusive process, we have estimated the mutual diffusion coefficient D_{12}^*. To do so, we have used the fact that in an ideal solution the mutual diffusion coefficient can be obtained from [39]

$$D_{12}^* = x_1 x_2 \left(\frac{1}{x_1 M_1} + \frac{1}{x_2 M_2} \right)^2 (x_2 M_2)^2 \frac{N(\langle \Delta r_{c.m.}^* \rangle)^2}{6t^*}, \quad (21)$$

where N is the total number of particles, t^* is the time and $\Delta r_{c.m.}^*$ is the mean-squared displacement of the center of the mass of all fluid molecules. Using this procedure, we have obtained $D_{12}^* = 0.32 \pm 0.05$.

Assuming a diffusion equation behavior, the configuration studied here leads to an evolution of the molar fraction that follows roughly [40]

$$x_1 = x_{1\text{-}statio.} \left[1 - \exp\left(- \frac{t^*}{\theta^*} \right) \right], \quad (22)$$

where $x_{1\text{-statio}}$ is the stationary molar fraction and $\theta^* = h^{*2}/(\pi^2 D_{12}^*)$ is the diffusion characteristic time. A more refined solution of this problem leads to [41]

$$x_1 = x_{1\text{-}statio.} \left[1 - \frac{8}{\pi^2} \exp\left(- \frac{t^*}{\theta^*} \right) \right]. \quad (23)$$

It should be noted that both relations are not appropriate to deal with very short times [41].

From Fig. 12, it appears that Eqs. (22) and (23) represent very well the transient behavior computed by MD simulations. Thus, we can conclude that the establishment of the

TABLE II. Ternary and ten-component thermal diffusion factors of each compound, using Eq. (20) as the one fluid approximation on mass.

Mixture	α_{T1}	α_{T2}	α_{T3}	α_{T4}	α_{T5}	α_{T6}	α_{T7}	α_{T8}	α_{T9}	α_{T10}
Ternary	1.75	−0.15	−1.61							
Decanary	1.44	1.03	0.65	0.30	0	−0.27	−0.5	−0.71	−0.89	−1.05

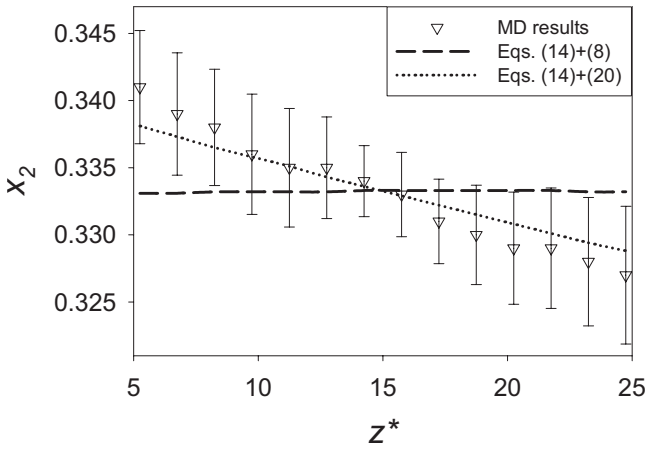

FIG. 11. Nonisothermal ($\Delta T^*/h^* = 15.9 \times 10^{-3}$) molar fraction segregated profiles of the component 2 in a ternary isotopic mixture.

gravitational segregation (isothermal or not) follows a diffusionlike process guided by the mass diffusion coefficient. This result is important as it emphasizes that a macroscopic dynamic model aiming to describe the gravitational segregation process [6,7] should be formulated in such a way that its transient behavior is conducted by the mass diffusion.

IV. CONCLUSIONS

In this work, for the first time ever to the best of our knowledge, a molecular dynamics algorithm is proposed to study the transient and the stationary state of gravitational segregation in isotopic mixtures. Both isothermal and stable nonisothermal (where thermodiffusion occurs) cases have been studied. The fluid particles are described by Lennard-Jones spheres but the approach is extensible to any kind of molecular model. This work is aimed to deal with situations that resemble to those occurring in a stable petroleum reservoir composed of hydrocarbons subjected to a geothermal gradient.

In the first part, simulations have been performed on binary equimolar mixtures (with $M_2/M_1 = 10$) for various gravity amplitudes. It has been found that, discarding the areas close to the walls for the analysis, the MD simulation stationary results are in perfect agreement with the analytical solution of the thermodynamic modeling for $T^* = 2$ and $\rho^* = 0.6$. Then, simulations have been performed for various thermodynamic conditions including the biphasic case. In all cases, MD simulation results have been found to be consistent with the thermodynamic modeling showing an influence of the temperature, but not of the density, on the stationary concentration profiles.

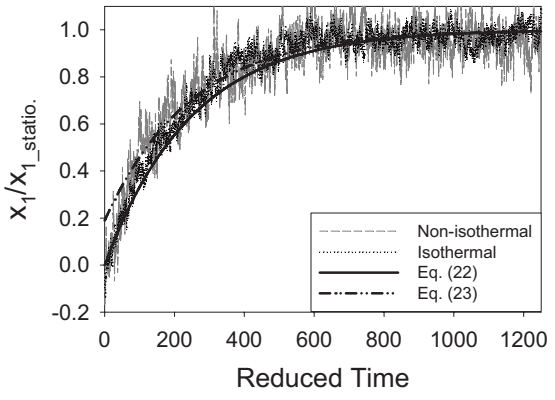

FIG. 12. Evolution of the molar fraction during gravitational segregation in a binary equimolar isotopic mixture ($M_2/M_1 = 10$) at $T^* = 2$ and $\rho^* = 0.6$ for $g^* = 0.02$.

Then, on the same mixture, MD simulations have been carried out in nonisothermal situations (heated from below) for different thermal gradients. It has been found that, because of the small height of fluid simulated (a few nanometers), the Rayleigh number is always largely below its critical threshold, i.e., the system is stable. Stationary simulations results have shown that the non-negligible influence of thermodiffusion on the composition profiles of the studied mixtures is opposite to the gravity one. The thermodiffusion effect can even reverse the composition distribution along the fluid column for a very large thermal gradient. In addition, it has been found that the MD compositions profiles are consistent with those predicted by an adequate thermodynamic modeling.

Next, ternary and ten-component isothermal and nonisothermal mixtures have been studied. As for the binary mixtures, it has been noticed that in the nonisothermal case, the stationary concentration profiles are modified in a noticeable manner by the thermodiffusion effect compared to the isothermal situation. This result confirms the importance of thermodiffusion when estimating the concentration profile in some petroleum reservoir. In addition, it has been demonstrated that a thermodynamic modeling of these multicomponent isotopic LJ mixtures can be performed using an *ad hoc* one fluid approximation. The usual linear one fluid model on mass is shown to be inadequate. Therefore, an empirical one fluid model is proposed that ensures the consistence of the thermal diffusion factor values.

Finally, the transient behavior of isothermal and nonisothermal segregation in a binary mixture has been studied by MD simulations. The results have clearly shown that the evolution of the molar fraction in a given slab is similar to the one deduced from a diffusion equation. More precisely, it has been found that this segregation process, isothermal or not, follows a diffusion process based on the mutual diffusion coefficient. This firmly confirms that the macroscopic dynamic modeling of the gravitational segregation in multicomponent mixtures should be formulated in such a way that the transient behavior is guided by the mass diffusion coefficients.

ACKNOWLEDGMENTS

We gratefully acknowledge computational facilities provided by TREFLE laboratory, whose supercomputer has been financially supported by the Conseil Régional d′ Aquitaine. We thank Stephanie Delage-Santacreu and Jean-Paul Caltagirone for fruitful discussions.

[1] B. H. Sage and W. N. Lacey, Trans. AIME **132**, 120 (1939).
[2] F. Montel and P. L. Gouel, paper SPE 14410 presented at the SPE Annual Technical Conference and Exhibition, Dallas (1985).
[3] C. Lira-Galeana, A. Firoozabadi, and J. M. Prausnitz, Fluid Phase Equilib. **102**, 143 (1994).
[4] L. Høier and C. H. Whitson, SPE Reservoir Eval. Eng. **4**, 525 (2001).
[5] B. Wilbois, G. Galliero, J.-P. Caltagirone, and F. Montel, Philos. Mag. **83**, 2209 (2003).
[6] K. Ghorayeb, A. Firoozabadi, and T. Anraku, SPEJ **8**, 114 (2003).
[7] F. Montel, J. Bickert, A. Lagisquet, and G. Galliero, J. Pet. Sci. Eng. **58**, 391 (2007).
[8] N. Bakhtiari Nia and K. Movagharnejad, Fluid Phase Equilib. **262**, 174 (2007).
[9] S. Wiegand, J. Phys.: Condens. Matter **16**, R357 (2004).
[10] A. Leahy-Dios and A. Firoozabadi, J. Phys. Chem. B **111**, 191 (2007).
[11] P. Blanco, P. Polyakov, M. M. Bou-Ali, and S. Wiegand, J. Phys. Chem. B **112**, 8340 (2008).
[12] J. W. Gibbs, *Collected Works—Vol. 1—Thermodynamics* (Yale University Press, New Haven, 1957).
[13] S. Halldórsson and E. H. Stenby, Fluid Phase Equilib. **175**, 175 (2000).
[14] P. W. Atkins and J. de Paula, *Physical Chemistry*, 7th ed. (W.H. Freeman & Co., San Francisco, 2001).
[15] S. R. de Groot and P. Mazur, *Nonequilibrium Thermodynamics* (Dover, New York, 1984).
[16] J. K. Platten and J. C. Legros, *Convection in Liquids* (Springer, New York, 1984).
[17] J. P. Larre, J. K Platten, and G. Chavepeyer, Int. J. Heat Mass Transfer **40**, 545 (1997).
[18] F. Montel, J.-P. Caltagirone, and L. Pebayle, *The Mathematics of Oil Recovery*, edited by P. R. King (Clarendon Press, Oxford, 1992).
[19] L. J. T. M. Kempers, J. Chem. Phys. **115**, 6330 (2001).
[20] G. Galliero, M. Bugel, B. Duguay, and F. Montel., J. Non-Equilib. Thermodyn. **32**, 251 (2007).
[21] J. P. Hansen and I. R. McDonald, *Theory of Simple Liquids* (Academic Press, London, 1986).
[22] M. Schoën, *Computer Simulation of Condensed Phases in Complex Geometries*, Lecture Notes in Physics No. M17 (Springer-Verlag, Berlin, 1993).
[23] F. Müller-Plathe, J. Chem. Phys. **106**, 6082 (1996).
[24] M. P. Allen and D. J. Tildesley, *Computer Simulation of Liquids* (Oxford Science, Oxford, 1987).
[25] H. J. C Berendsen, J. P. M. Postma, W. F. van Gunsteren, A. di Nola, and J. R. Haak, J. Chem. Phys. **81**, 3684 (1984).
[26] L. Verlet, Phys. Rev. **159**, 98 (1967).
[27] A. Parola, A. Meroni, and L. Reatto, Phys. Rev. Lett. **62**, 2981 (1989).
[28] G. Galliero, C. Boned, A. Baylaucq, and F. Montel, Phys. Rev. E **73**, 061201 (2006).
[29] G. Galliero, T. Lafitte, D. Bessieres, and C. Boned, J. Chem. Phys. **127**, 184506 (2007).
[30] J. M. Haile, *Molecular Dynamics Simulation: Elementary Methods* (Wiley, New York, 1992).
[31] F. Müller-Plathe, Phys. Rev. E **59**, 4894 (1999).
[32] G. Galliero, C. Boned, A. Baylaucq, and F. Montel, Fluid Phase Equilib. **234**, 56 (2005).
[33] M. Bugel and G. Galliero, Chem. Phys. **352**, 249 (2008).
[34] D. O. Dunikov, S. P. Malyshenko, and V. V. Zhakhovskii, J. Chem. Phys. **115**, 6623 (2001).
[35] D. C. Rapaport, Phys. Rev. E **73**, 025301(R) (2006).
[36] R. Piazza and A. Parola, J. Phys.: Condens. Matter **20**, 153102 (2008).
[37] G. Galliero and S. Volz, J. Chem. Phys. **128**, 064505 (2008).
[38] G. Galliero, B. Duguay, J. P. Caltagirone, and F. Montel, Philos. Mag. **83**, 2097 (2003).
[39] D. L. Jolly and R. J. Bearman, Mol. Phys. **41**, 137 (1980).
[40] E. L. Cussler, *Diffusion: Mass Transfer in Fluid Systems* (Cambridge University Press, New York, 1997).
[41] J. A. Bierlein, J. Chem. Phys. **23**, 10 (1955).